AD-A045 667 GENERAL ELECTRIC CO SYRACUSE N Y ELECTRONICS LAB F/G 20/6
PRACTICAL APPLICATION OF HOLOGRAPHIC INTERFEROMETRY,(U)
OCT 68 D E DUFFY
UNCLASSIFIED R68ELS-93 NL

1 OF 1
ADA
045667

END
11-77
DDC

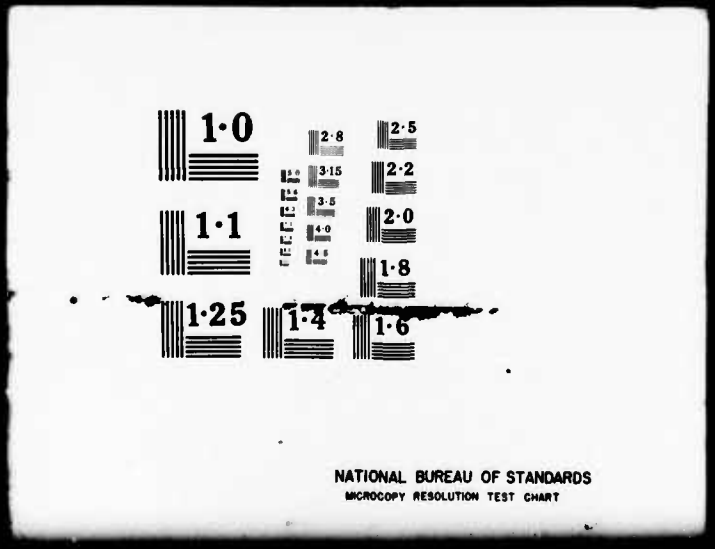

ELECTRONICS LABORATORY • SYRACUSE, N.Y.

(1)

AUTHOR	SUBJECT	TIS Nº
(10) D. E. Duffy	Holography	(14) R68ELS-93
		DATE
		(11) October 1968

TITLE	GE CLASS
(6) PRACTICAL APPLICATION OF HOLOGRAPHIC INTERFEROMETRY	1
	GVT CLASS
	None

REPRODUCIBLE COPY FILED AT TECHNICAL INFORMATION EP13	ELECTRONICS LABORATORY SYRACUSE, N.Y.	Nº OF PAGES
		49

(12) 65p.

SUMMARY

Holographic interferometry offers great potential as a method for detecting small changes in any type of three-dimensional object. This report indicates several possible areas of application. Numerous photographs are included to demonstrate the use of this technique for observing resonant modes in various types of vibrating objects, for comparing differences between an object in its distorted and undistorted state, and for observing refractive index changes due to air flow around an object.

The appendix discusses the relationships between recording and reconstruction parameters in a holographic system.

KEY WORDS 3-D Display, Holography, Interferometry, Optics, Vibration Analysis

INFORMATION PREPARED FOR Electronics Laboratory

WORK CONDUCTED BY Author

APPROVED William A Penn (SS Mgr) / [signature] (Sect Mgr)

-A-

149508

TABLE OF CONTENTS

LIST OF ILLUSTRATIONS

LIST OF ILLUSTRATIONS (concluded)

I. INTRODUCTION AND REVIEW

This report illustrates several possible areas of application of holographic interferometric techniques for measurement of small changes in a three-dimensional object or volume of space. Hologram interferometry has been described in the literature by various authors.[1, 2] Briefly, the technique consists of comparing the image of an object reconstructed from a hologram[3, 4] with the object itself (or a second image of the object) after the object has undergone some type of change.

Because of the ability of a hologram to precisely reconstruct the wavefronts that were stored in it, holographic interferometry differs from classical interferometry in two basic aspects. First, it can be used to compare the wavefronts from a three-dimensional diffusely reflecting or transmissive object. Classical interferometry, on the other hand, is limited to the comparison of the deviations of known plane or spherical wavefronts after reflection or transmission from a highly specular object. Secondly, hologram interferometry permits comparison of two wavefronts occurring at completely different intervals of time.

There are three general classes of hologram interferometry, usually designated (1) real-time interferometry, (2) double exposure interferometry, and (3) time average interferometry. In the real-time interferometry, a hologram of some object is recorded and, after processing, the hologram is precisely positioned in the same place where it was recorded, so that, when it is illuminated, the image from the hologram falls exactly on the object. The object and the hologram are then both illuminated exactly as they were when the hologram was recorded. Since the light waves from the hologram are exactly like those from the object, the wavefronts are in phase and there are no interference fringes produced. This is the so-called zero-beat or null condition. If, now, the object is caused to undergo some change, say due to some stress or strain, or vibration, the light wave from the object differs from the wave from the hologram image. At those points on the object where the light path from the object differs from that of the hologram image

by an integral multiple of a half wavelength, interference fringes are produced. Where the path difference is an integral multiple of a wavelength, one observes a bright fringe, and at odd half multiples of a wavelength, one observes a dark fringe. These fringes then represent contours of constant displacement over the object. More precisely, this path difference is the "optical path difference" and not simply the geometric path difference, since the object need not be an opaque object, but could be transparent, as in the case of a lens or volume of gas in which the refractive index is changed. Since the wavelength of light is approximately 0.5 microns and each fringe represents an optical path difference of $\lambda/2$ between the object and image, one can obtain very fine measurements on the changes that have occurred between the object and image. Qualitative measurements require a knowledge of the optical system layout during recording, reconstruction, and viewing of the fringe patterns. Fringe interpretation is discussed later.

Real-time holographic interferometry is particularly useful for analyzing phenomena that change with time, such as airflow patterns around some obstacle, gas flow out of a jet nozzle, changes in refractive index in a gas or transparent material due to temperature changes. It is presently finding application in the analysis of vibrating objects such as sonar transducers, loud speakers, and turbine blades. It permits one to see the intricate mode patterns while the object is in motion and allows one to change the driving frequency or displacement amplitude at will. It permits a quick gross analysis of various types of vibrations that can occur in a body of any shape.

The "real time" interferometry is perhaps the most difficult to perform, since one must precisely position the hologram image back on the object. Double exposure hologram interferometry is easier to perform and is applicable where one wishes to compare an object (or volume of space) with itself after it has undergone some type of change; for example, to compare the object with itself after it has undergone some type of expansion or contraction. In the double exposure hologram, one exposure is made while the object is undistorted. Then, without moving the hologram plate, a second exposure is made, on the same plate, of the object in its distorted condition. After development, the hologram is illuminated by the reference wave, and both the undistorted and distorted images of the object are reconstructed. The two reconstructed wavefronts produce interference and the resultant fringe pattern shows the distortion.

This type of hologram has the advantage, over the real-time hologram, of not requiring precise replacement of the hologram in order to view the interference pattern; however, it has the disadvantage that a separate hologram must be made for each different pattern one wishes to view.

The time-average hologram is an extension of the double-exposure hologram and can be considered a multiple-exposure hologram. It is applicable where the object is undergoing some type of harmonic motion during the exposure. A detailed analyses of this type of hologram can be found in the literature. This hologram may be considered to be made up of a number of holograms of the object in each of its different positions. All of the images add together coherently to produce the resultant interference pattern. Obviously, the points that are not moving, or nulls, interfere constructively and produce bright fringes. In such harmonic motion, the two "dwell" points that represent the maximum positive and negative excursions are more heavily weighted than other positions in the motion, and the resultant fringe pattern represents contours of constant amplitude of vibration.

While each dark fringe represents an optical path difference of $\lambda/2$, the interpretation of the fringe patterns in holographic interferometry, particularly for diffusely reflecting objects, can be rather complex. Any point on a diffuse object can be viewed at a number of different angles, depending on the extent of the viewing window and, when viewing a point on the object and its corresponding displaced image point, the difference in optical path of the light from the two points becomes a function of the viewing angle. Thus, as one moves one's head around, the fringe pattern changes.

One of the simpler types of patterns to interpret occurs when the motion or displacement of the object is normal to the surface and both the viewing point and illuminating points are also essentially normal to the surface. A displacement of a point on the object of a $\lambda/4$ with respect to its image then corresponds to a path difference of $\lambda/2$ between light from the object and the corresponding image point, and a dark fringe occurs. Dark fringes occur for any displacement of an odd multiple of a quarter wave. Similarly, bright fringes occur for any even mutliple of a quarter wavelength. By counting the number of fringes between a known stationary point, or bright node and some other point on the object, and by multiplying by $\lambda/4$, the displacement of the point on the surface can be determined. A more rigorous treatment of fringe

pattern interpretation can be found in the literature,[1, 2, 5] and will be further described in a future T. I. S. As indicated earlier, the purpose of this report is simply to illustrate possible areas of application of holographic interferometry.

II. EXAMPLES OF HOLOGRAPHIC INTERFEROMETRY

One of the most promising areas of application of holographic interferometry is in the analysis of various types of vibration phenomena. The holographic technique permits analysis of any type or shape of body, allows quick gross analyses of the displacement patterns, or if desired, precise analysis, and it does not require the attachment or imposition of any measuring devices which might, in some manner, alter the type of motion of displacement.

Figure 1 shows a typical arrangement for recording a hologram. The laser is off to the left and is not shown in the picture. The laser beam passes through the microscope objective shown at the left in the photograph. The objective expands the laser beam to illuminate the object and reference mirror. The object, in this case, is a sonar transducer mounted in a V-block. Attached to the block on the right is the reference mirror. The hologram plate holder is shown in front of the transducer.

Figure 2 is a picture of the image produced by a hologram of the stationary transducer. The two pieces of cement on the surface of the transducer are points where the leads were attached. Time-average holograms were taken of the transducer while it was vibrating at various frequencies and voltage drive amplitudes. The design frequency of the bender is 3.68 kHz. Figure 3 shows several of the vibration mode patterns of this transducer taken at the design frequency, but with increasing drive voltage. The motion of the bender was normal to the surface. The illumination and viewing point were also essentially normal to the surface. Note that there are no fringes on the V-block or outside edges of the bender; these are null points. By counting the number of bright and dark fringes from a null and multiplying by $\lambda/4$, the displacement of any point on the bender fan be determined. This is the total excursion of a point from its maximum positive to negative positions. Note that the motion of the

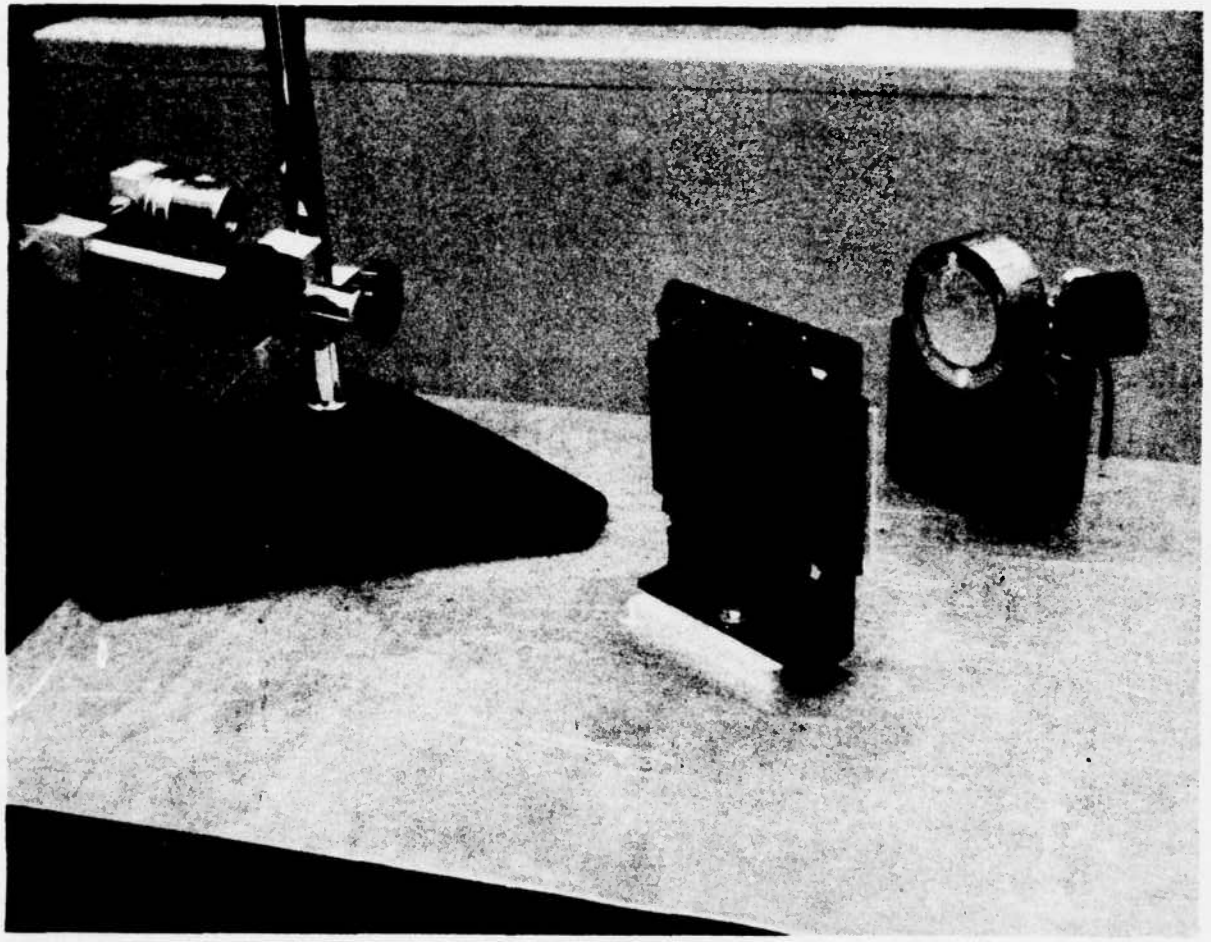

Figure 1. Arrangement for Recording Holograms of Transducer

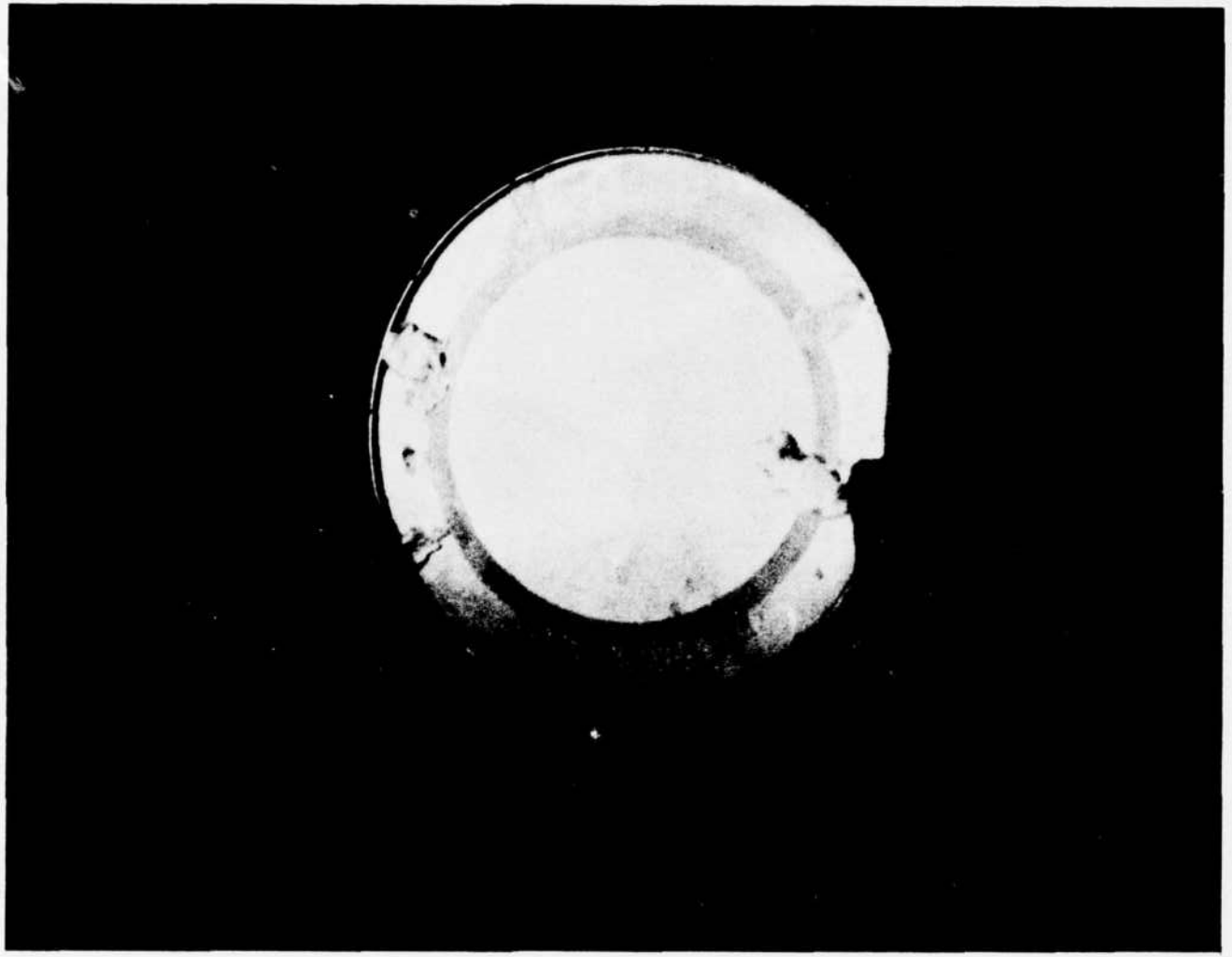

Figure 2. Reconstruction of Stationary Bender

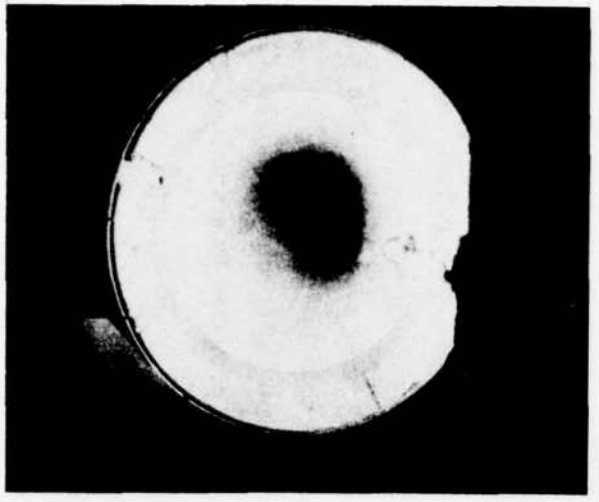

zero db

19 db

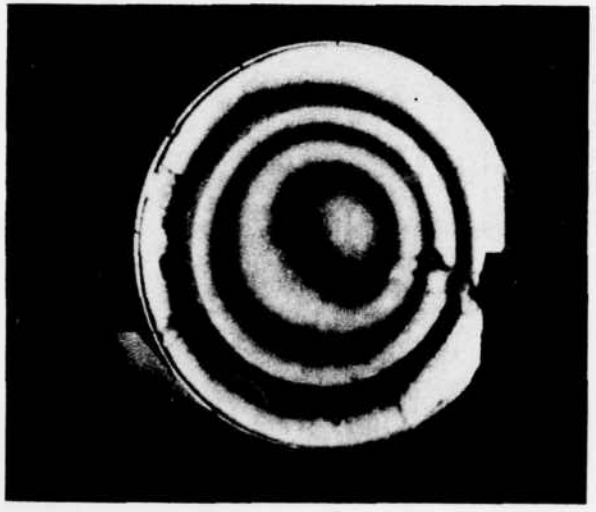

20 db

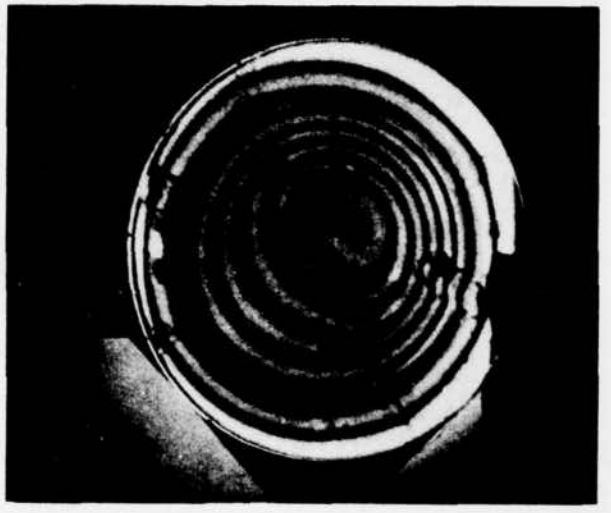

30 db

Figure 3. Fringes Produced by Increasing Motion at 3.68 kHz

surface is not symmetrical about the center of the bender. Figure 4 shows this was not due to the way the transducer was set in the V-block or the method of viewing. Here, the transducer was rotated 90° and it can be seen that the fringe pattern also rotated 90°. Figure 5 shows an overtone resonance in the bender at 17 kHz.

Figures 5 through 8 show the vibration patterns from another transducer. This was similar to the previous bender, except that it was potted. That is, the surface is encased, essentially, in a rubber type of cement. Figure 6 shows the reconstructed image of the stationary potted bender. Figure 7 shows several of the resonant patterns produced by increasing motion in the potted bender at 3.68 kHz. Note that the motion here is not the same as in the previous bender for the same frequency and drive voltage. For some reason, the potting material lowered the fringe constrast. However, it was found that, by covering the surface with masking tape, the fringe contrast could be enhanced without any noticeable change in the fringe pattern. Figure 8 shows the fringes produced in the potted bender at 15 kHz, in which the upper half of the surface was covered with masking tape but the lower half was not covered. Note the increased contrast.

Figures 9 through 11 illustrate the vibration fringes produced in a more complex object. The object consisted of a small model of a rocket. The rocket was caused to vibrate by a small electromagnet placed behind the rocket. At the left in Figure 9 an ordinary photograph of the rocket is shown, and at the right, the image of the rocket is shown reconstructed from a hologram. The large threaded screw is part of the C-clamp used to hold the driving coil. Figure 10 shows the vibration fringes produced at three different resonant frequencies. Figure 11 shows the interference patterns produced by a small spacecraft model vibrating at 400 cycles per second.

All the preceding interferograms were obtained from time-average hologram interferometry. The following examples illustrate the use of double-exposure interferometry. The object again consisted of the rocket model, but this time the model was distorted by placing a small weight on top of the rocket. First, a hologram of the rocket in its undistorted state was recorded. Then, a weight was set on top of the rocket and a second exposure was recorded on the same holographic plate. The hologram then reconstructs both images, which beat together to produce an interference pattern that reveals the distortion.

3.68 kHz 30 db

Figure 4. Fringes Produced with Transducer Rotated 90 Degrees

Figure 5. 17 kHz Overtone Resonance in Bender

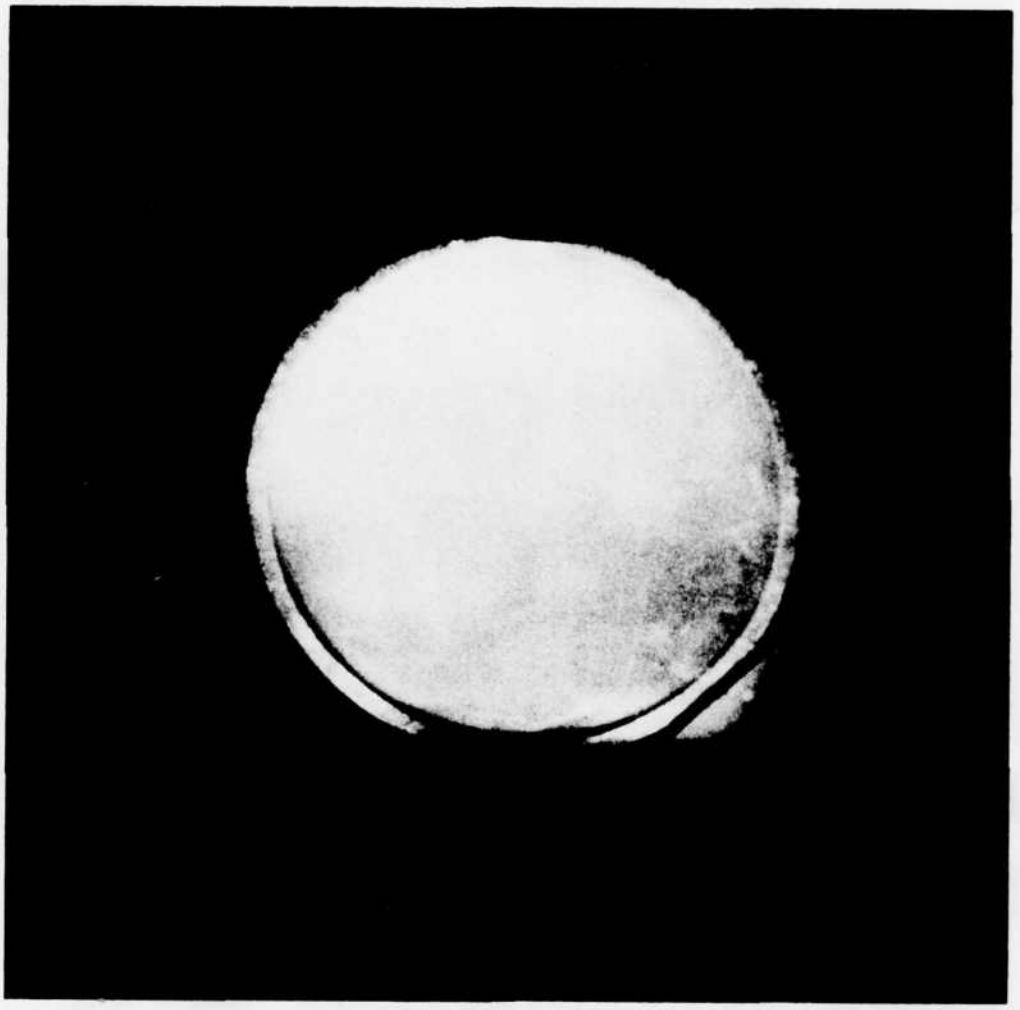

Figure 6. Reconstruction of Stationary Potted Bender

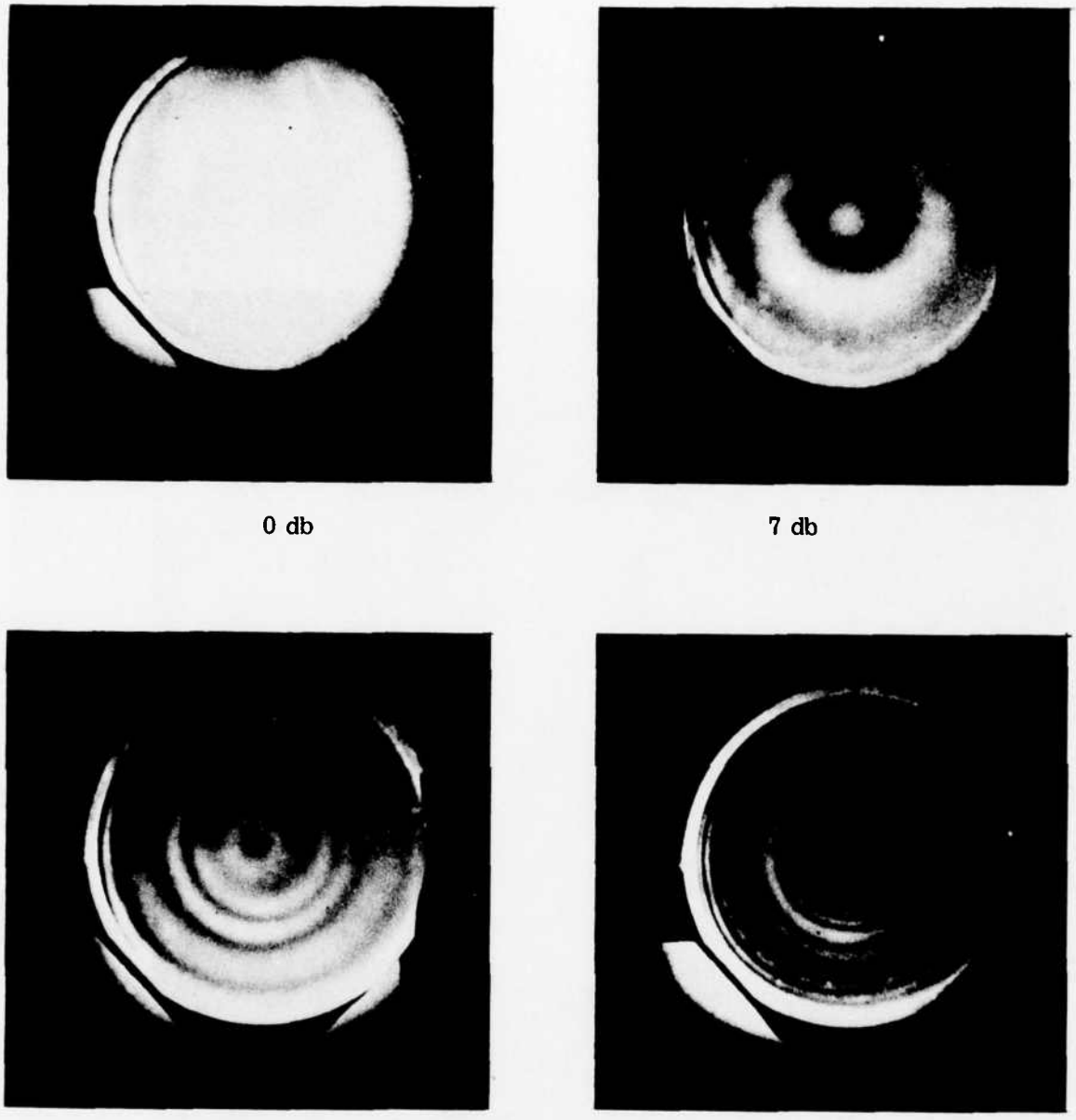

Figure 7. Fringes Produced by Increasing Motion in Potted Bender at 3.68 kHz

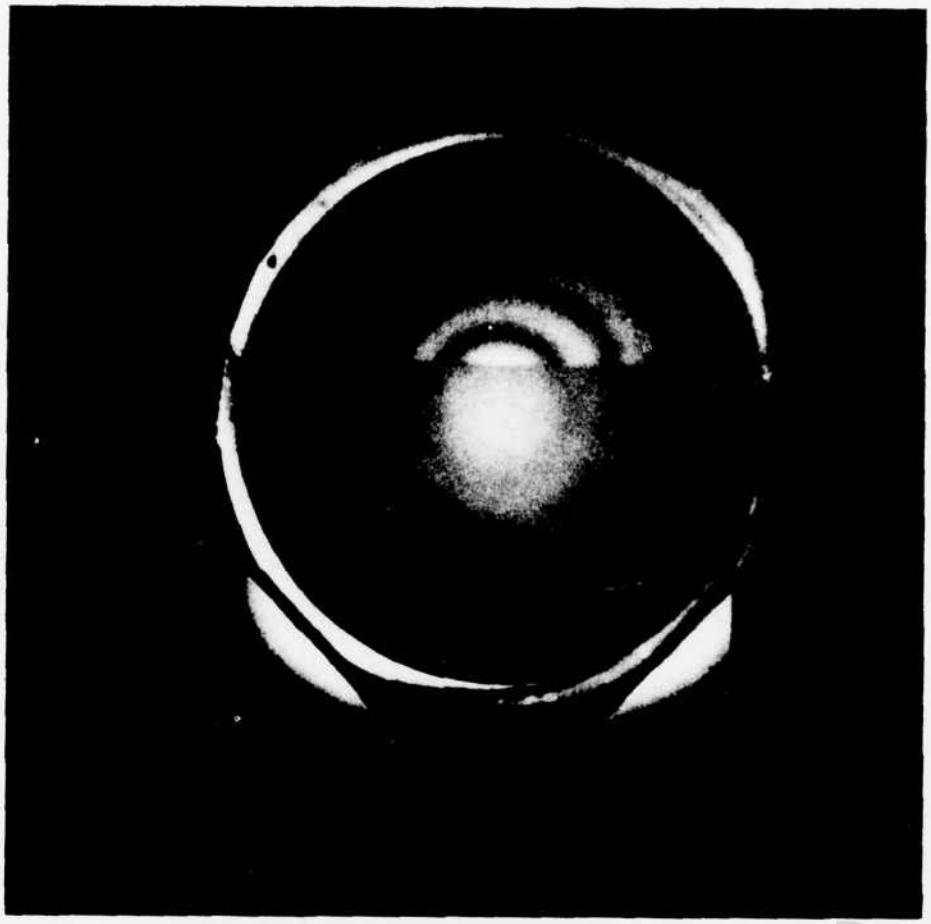

Figure 8. Fringes Produced in Potted Bender at 15 kHz

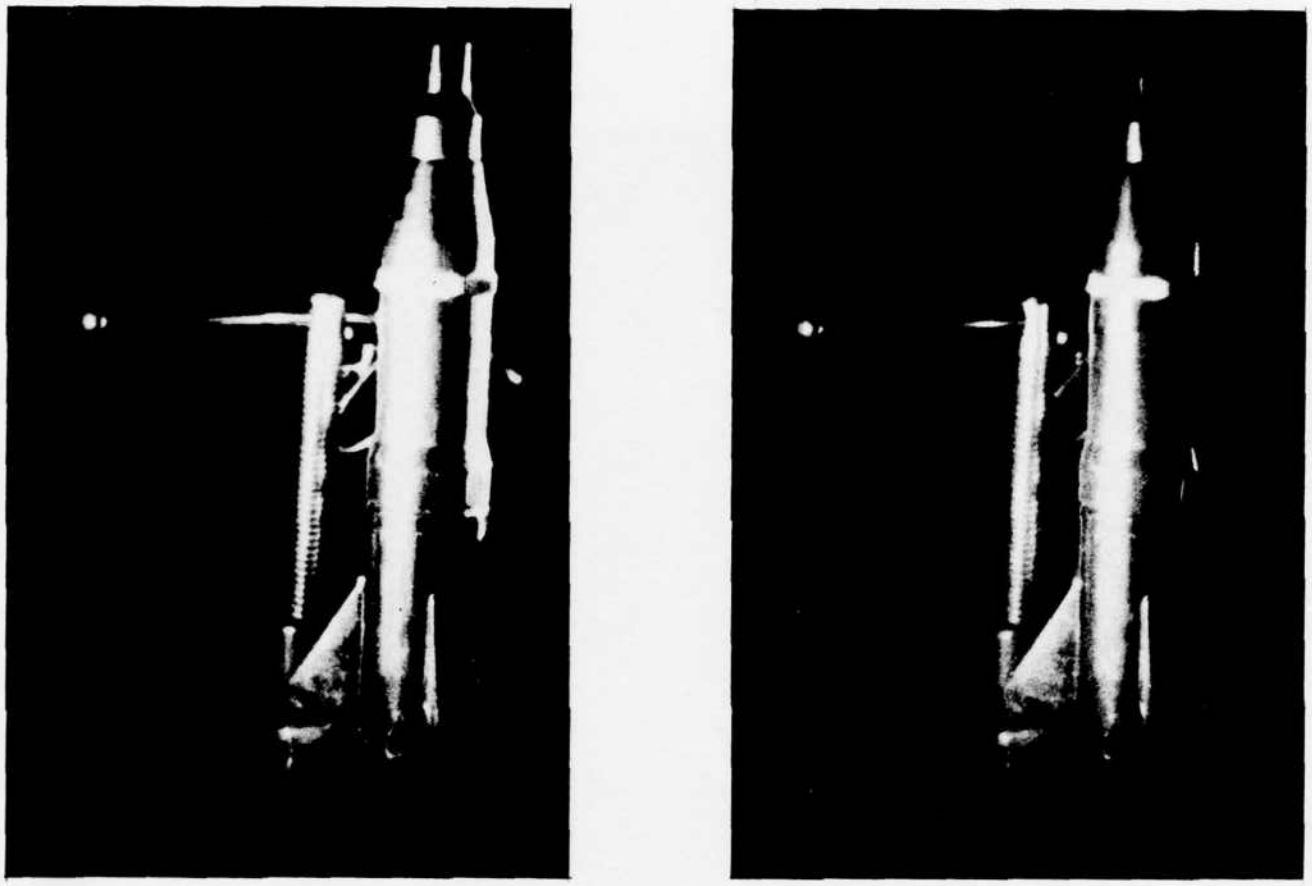

Figure 9. Ordinary Photograph and Holographic Reconstruction of Rocket Model

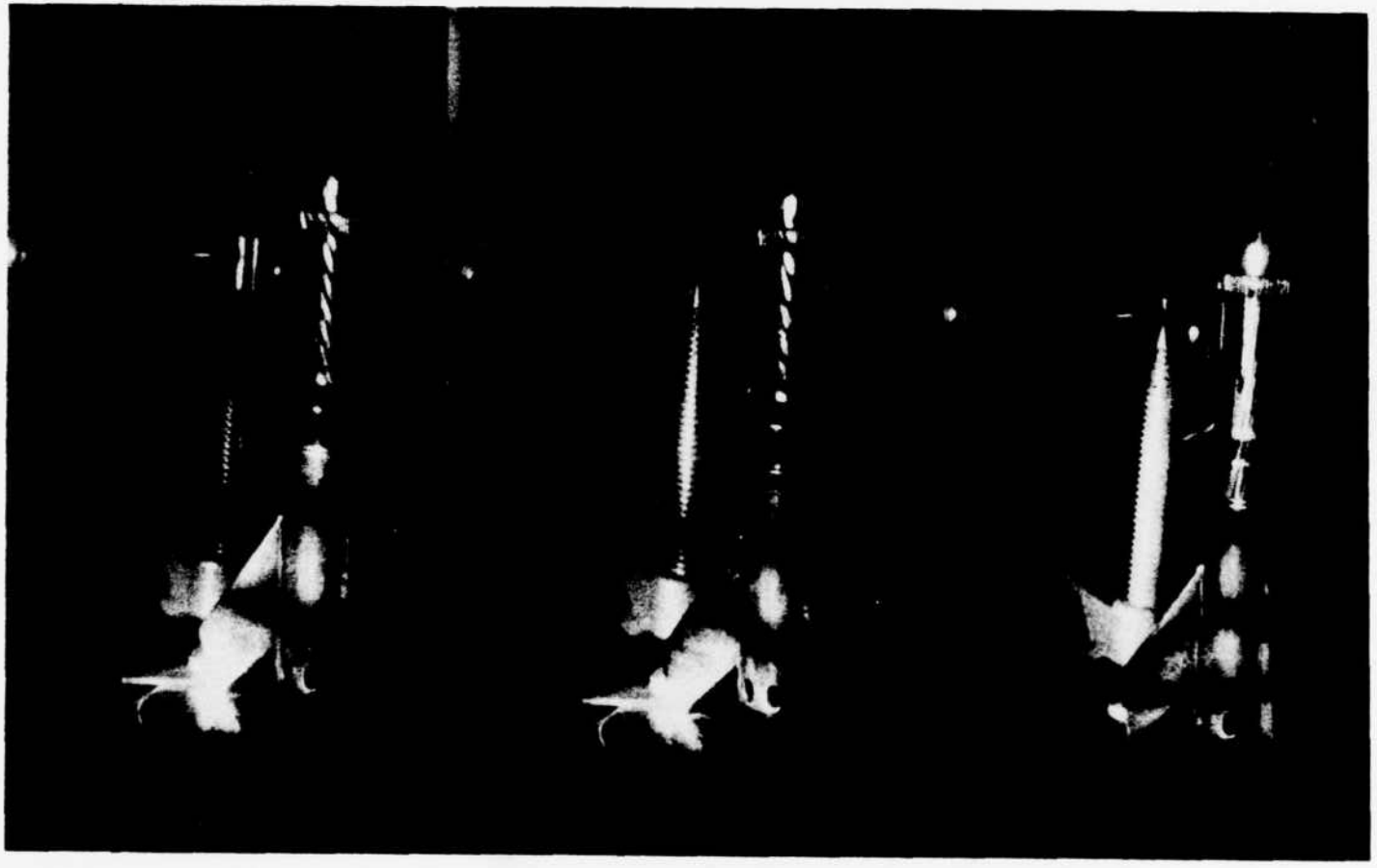

100 cycles/ sec. 270 cycles/sec. 450 cycles/sec.

Figure 10. Interference Fringes Due to Vibrating Rocket

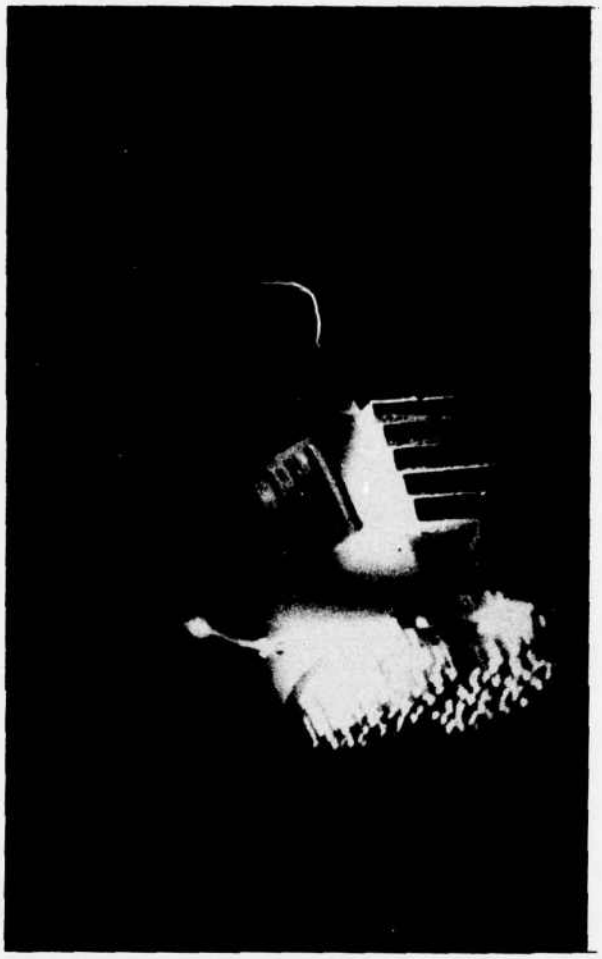

Figure 11. Space Craft Vibrating at 400 Cycles/sec.

Weights of three different sizes were used. These are shown in Figure 12. Placing the weights on top of the rocket caused it to be compressed. The interference fringes indicating the displacement due to each weight are shown in Figure 13. Note the decrease in the number of fringes as the weight decreases. There are very fine fringes at the tip of the rocket, which cannot be seen in the photographs but which appear in the holographic image when viewed with a high-power magnifier. In the photograph where the 0.25 gm weight was used, there is one dark fringe in the center of the rocket and the fine fringes near the top can be resolved without a magnifier. Figure 14 shows the interference fringes produced when the 11.82 gm weight was attached to one of the bottom fins of the rocket. This caused the bottom of the rocket to twist.

Figures 15 and 16 illustrate the use of double-exposure holographic interferometry for observing air-flow patterns. The air flow was produced by a hot soldering iron. First, an exposure was made while the soldering iron was cool. A second exposure was then recorded on the same film plate when the iron was hot. Typical fringe patterns around the tip of the soldering iron are shown in Figure 15. Figure 16 shows the air flow patterns produced by blowing on the tip of the hot soldering iron.

As illustrated by the previous examples, holographic techniques are very sensitive to small displacements on an object. While this provides a sensitive measuring technique, it can be a very serious problem when trying to record a hologram of some three-dimensional scene. Recording a hologram generally requires very-high-resolution film, and the films used are very slow compared to those used in ordinary photography. The exposure time, of course, depends on the output energy of the laser used to illuminate the object. Normally, Ne-He lasers are used for illumination and the exposure is on the order of many seconds to several minutes. Any motion of the object during the exposure either washes out the image completely, or produces interference fringes on the reconstructed image. For this reason, holographic recording generally requires very stable equipment. Figure 17 shows the reconstructed image of a model spacecraft that was resting on a granite table floating on rubber inner tubes. The table was on the second floor of the building and the exposure time was five minutes. Room vibrations transmitted through the table caused the model to move during the exposure and produced the dark interference fringe seen in the photograph of the reconstructed image.

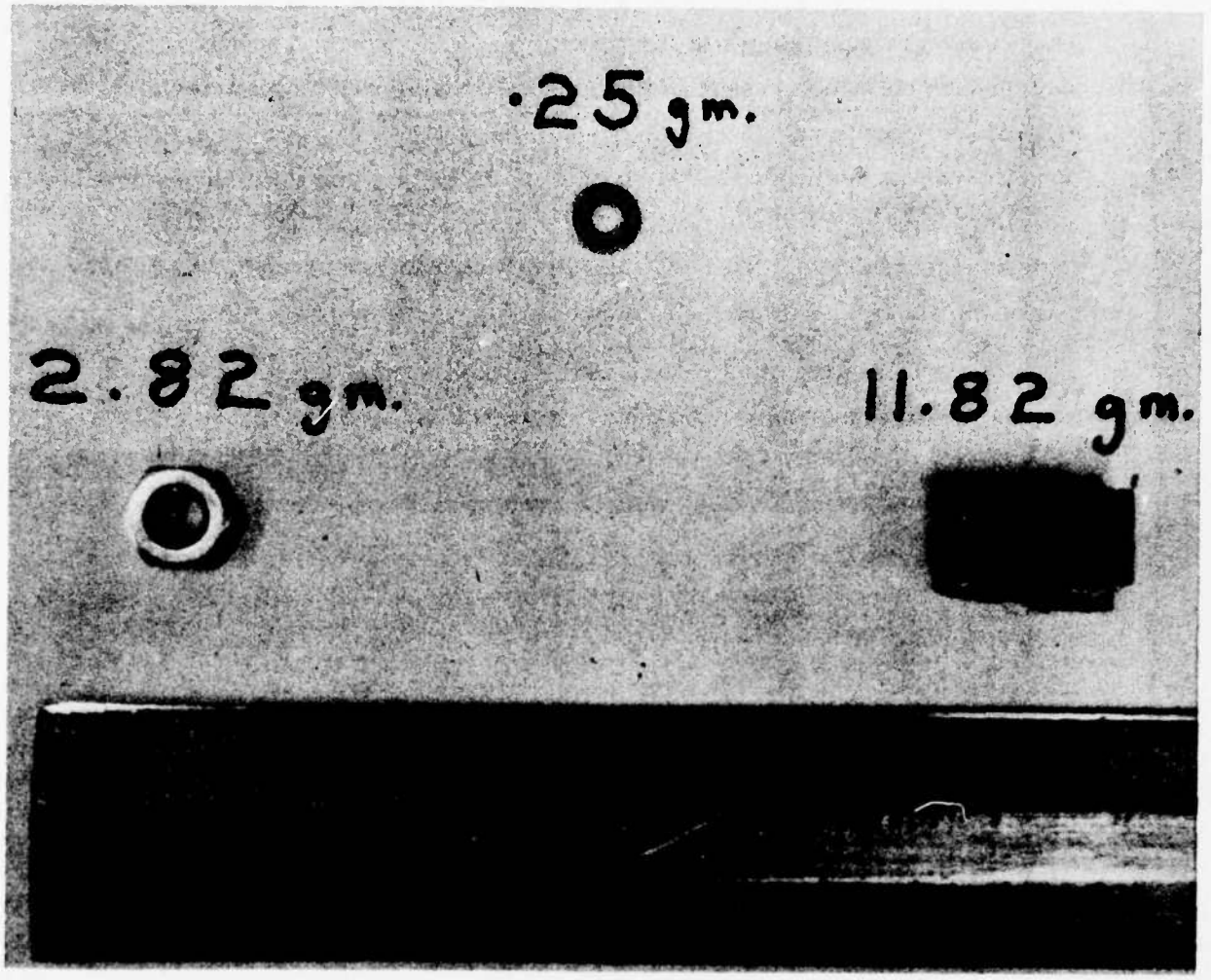

Figure 12. Weights Placed on Rocket

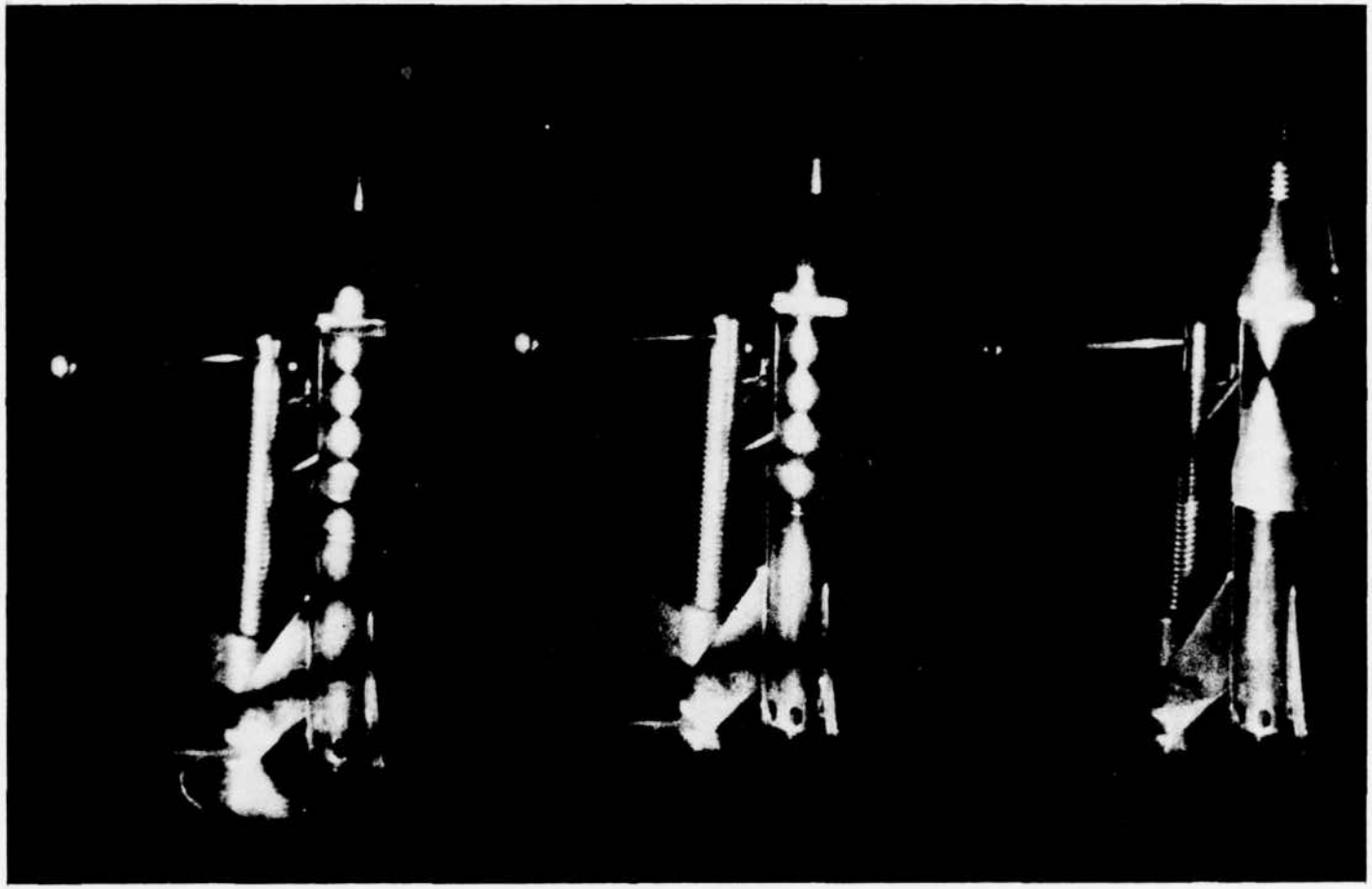

11.82 grams 2.82 grams 0.25 grams

Figure 13. Fringes Indicating Displacement Due to Weight on Top of Rocket

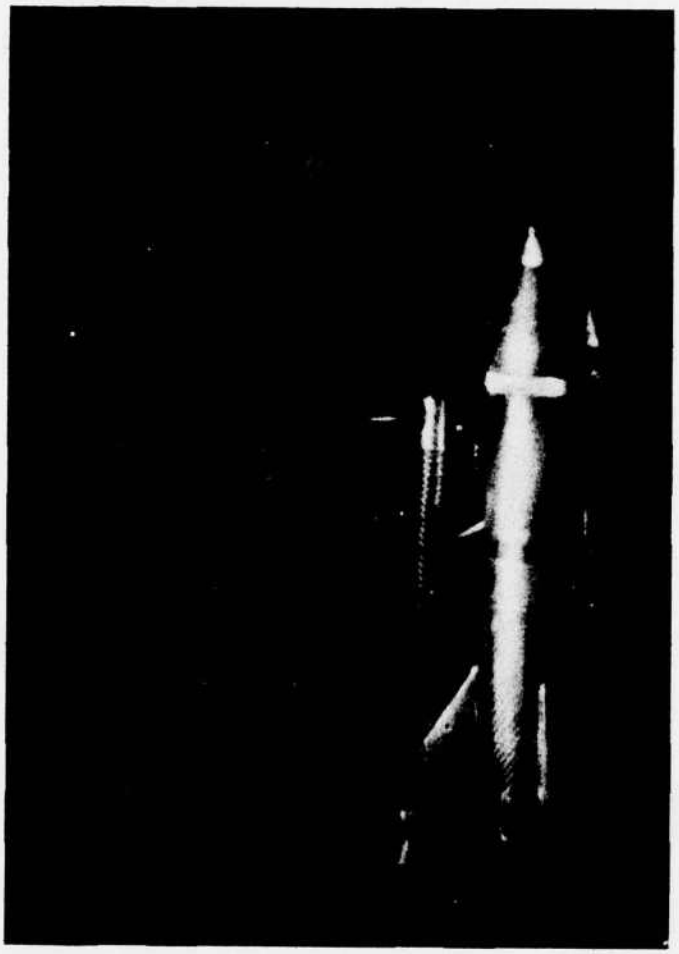

Figure 14. Fringes Due to 11.82 Gram Weight Attached to Fin of Rocket

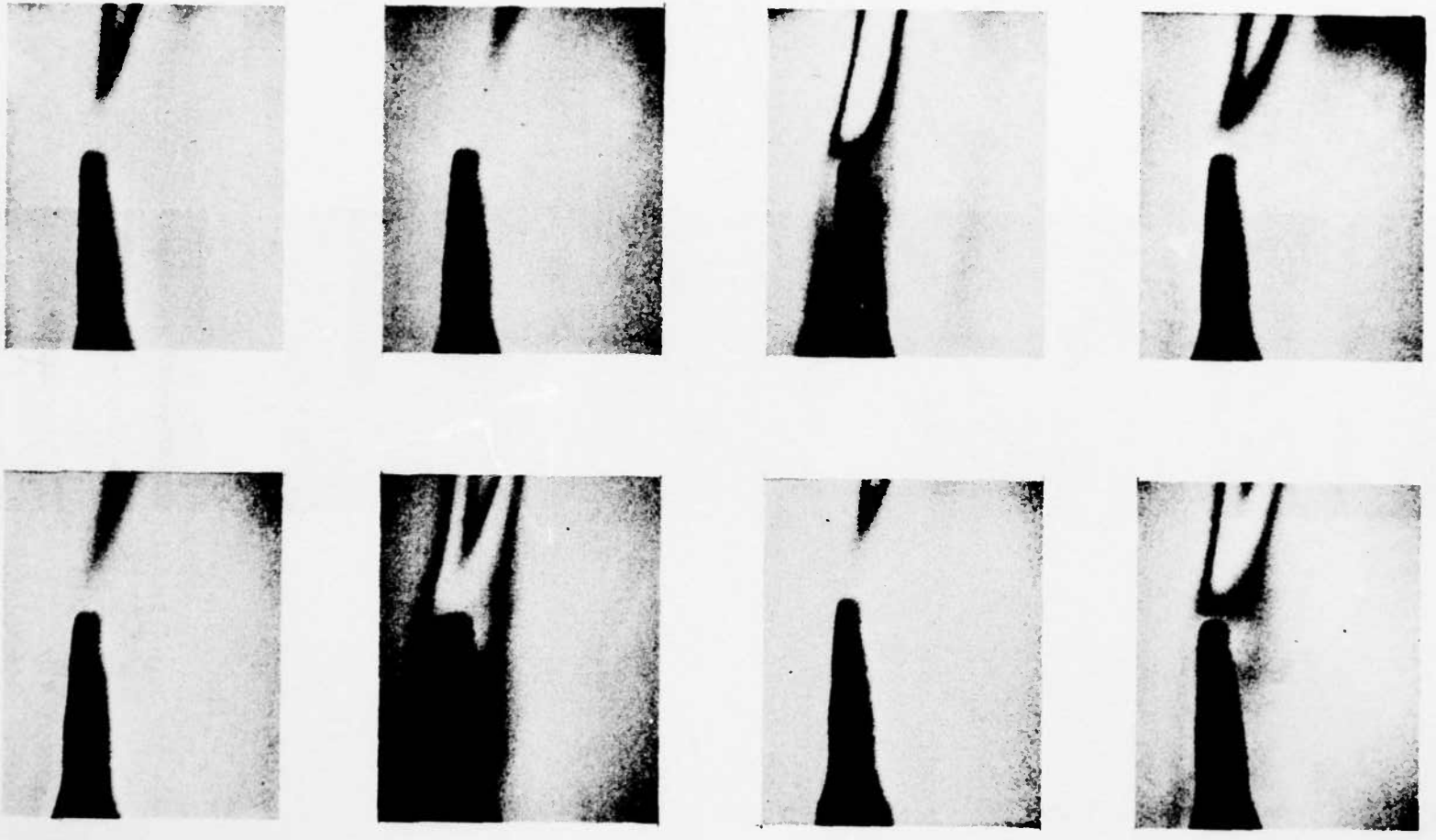

Figure 15. Air Flow Patterns at Tip of Hot Soldering Iron

Figure 16. Air Flow Patterns Due to Blowing on Tip of Hot Soldering Iron

Figure 17. Reconstruction of Model Space Craft

As in classical interferometry, the interference fringes are not necessarily situated on the surface of the reconstructed image, but may be localized some distance in front of, or behind, the image. This is illustrated in Figure 18, which is a double-exposure hologram in which the film plate was moved slightly between exposures. In photographing the reconstructed image, the lens aperture was wide open, so that the depth of field was very short. The camera was first focused on the rocket and then the focus gradually changed to positions behind the rocket. Note that the fringes do not become sharp until the camera is focused about 15 ft. behind the rocket. Interpretation of the fringe pattern when it is not situated near the object, of course, becomes impractical. However, it can be shown that, by sufficiently narrowing down the viewing aperture, the fringes can be localized near the surface of the object.

III. SUMMARY

Holographic interferometry offers great potential as a method for detecting changes in any type of three-dimensional object. The examples shown illustrate only a few of the many areas in which the technique can be used. It permits observation in real time, in which gross measurements can be made, or if desired, extremely precise measurements can be made. It does not impose any outside constraints on the object that might somehow alter the motion or type of change the object is undergoing. The changes in the object may be due to vibrating motions, static stresses or strains set up in the object, changes of refractive index, or degree of polarization of the object.

Focus 2 ft . on rocket | 2 ft . on screw | 4 ft. | 5 ft.

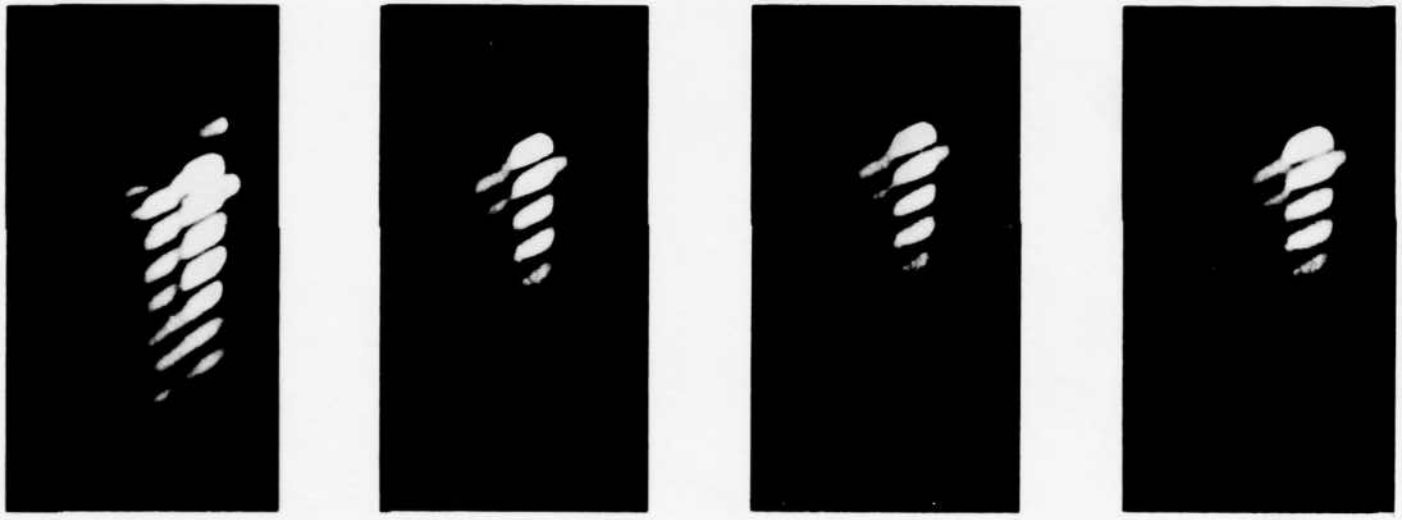

Focus at 7 ft . | 10 ft. | 15 ft. | infinity

Figure 18. Fringes Due to Motion of Hologram Plate

REFERENCES

1. R. L. Powell, K. A. Stetson, J. Opt. Soc. Am., 55, (1965), p. 1953.
2. B. P. Hildebrand, K. A. Haines, Appl. Opt., 6, (1966), p. 172.
3. E. Leith, J. Upatnicks, J. Opt. Soc. Am. 54, p. 1295, Nov. 1964.
4. D. Duffy, Optical Pattern Recognition and Holography, 1966, G. E., R66ELS-106.
5. L. W. Orr, S. W. Tehon, N. E. Barnett, Applied Opt. 7, (1968), p. 202.
6. G. L. Rogers, Nature, p. 237, Aug. 1950.
7. E. Leith, J. Upatnicks, K. Haines, JOSA, 55, p. 981, 1965.
8. Intensity Distribution in the Neighborhood of Focus of a Fresnel Zone Plate, D. Duffy, G. E. TIS, R63ELS-6.
9. Diffraction Imaging Grating Techniques, Vol. 1, Tech. Doc. No. ASD-TDR-63-595, G. E. Co. Contract AF33(657)-8357, May 1963.
10. The Use of Photographic Film and Rapid Processing Techniques in Coherent Optical Systems, D. Duffy, G. E. TIS, R66ELS-77.

APPENDIX A
DESIGN EQUATIONS FOR HOLOGRAPHIC SYSTEMS

A. DISCUSSION OF RECORDING AND RECONSTRUCTION SYSTEMS

The reconstructed image produced by a hologram can have all of the aberrations that are associated with ordinary lenses, e.g., spherical abberration, coma, astigmatism, curvature of field, distortion, chromatic aberration, and different magnifications in the lateral and longitudinal dimensions. All of these effects must be taken into account in the design of a holographic system. In particular, a constant awareness of the results of these effects, and when they might occur, should be maintained in the interpretation of any data collected from a holographically reconstructed image. The need for an awareness and familiarity with the problems that can arise, both in recording and reconstructing the image, cannot be over-emphasized, if one is trying to obtain precise measurements on the image.

While there are numerous variations, holographic systems may be divided into two separate types. These are the on-axis reference-beam system and the off-axis, or tilted-reference-beam systems. In the on-axis system, the light that is scattered from the object combines with the light passing through, or around, transparent areas in the object, to produce an interference pattern which, when recorded, is called a hologram. In the off-axis reference beam system, a portion of the light beam used to illuminate the objects is deflected around the object by a system of mirrors and beamsplitters. It is then superimposed on the light scattered from the object at the recording plane, to produce the hologram.

The various relationships between object and image positions, magnification, and aberrations have been formulated and can be found in the literature. Some of these will simply be repeated here. However, a quasi-rigorous derivation of some of the more important factors is given, in what follows, to emphasize the inter-relationship of all of the effects. The operator of any holographic system should familiarize himself with what follows, in order to interpret the data collected.

B. BASIC PRINCIPLES OF HOLOGRAPHY

Figure A-1 is a sketch of the general arrangement for recording the hologram.

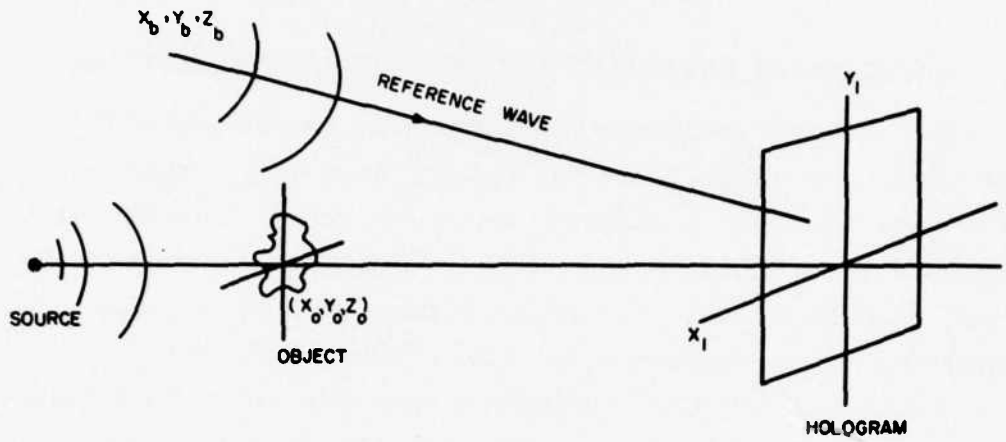

Figure A-1. Hologram Recording

The object is illuminated by a point source of coherent light of wavelength λ_1. Let the light distribution arriving at the hologram recording plane due to the object wave (either by reflection or transmission) be

$$U_o = A_o(x_1, y_1)\, e^{j\phi_o(x_1, y_1)}. \qquad (1)$$

where

U_o = complex light amplitude in hologram plane.
$A_o(x_1, y_1)$ = amplitude modulus.
$\phi_o(x_1, y_1)$ = phase in radians.
x_1, y_1 = lateral coordinates in hologram plane.

A portion of the light originating from the source illuminating the object is deflected around the object by a system of mirrors and beam splitters and

is combined with the wave from the object at the recording plane. This is called the reference or background wave and is designated as

$$U_b = A_b(x_1, y_1)e^{j\phi_b(x_1, y_1)}. \tag{2}$$

where subscript b refers to the reference wave.

These two waves being coherent combine amplitude-wise at the recording plane to produce a resultant intensity of

$$I = \left| U_o + U_b \right|^2 \tag{3}$$

Photographic film is a square law detector and senses intensity rather than amplitude. In order to reconstruct an image of the illuminated object the film must be exposed and processed such that the amplitude transmittance T of the film is linear with intensity. Assuming that there are no phase effects in the film, the amplitude transmission is the square root of the intensity transmission. The method of maintaining linearity during exposure and development of the film and the effects of non-linearities is discussed in Section H. For the moment assume the amplitude transmission of the film or hologram is linear with intensity and for simplicity let the amplitude transmission be

$$T = \left| U_o + U_b \right|^2 = U^2_o + U^2_b + U_o U^*_b + U_b U^*_o \tag{4}$$

where the starred terms represent the complex conjugate.

After appropriate exposure and processing the photographic film or hologram is re-illuminated with a coherent light source. The light distribution leaving the hologram is then

$$U = U_a [\, U^2_o + U^2_b + U_o U^*_b + U_b U^*_o] \tag{5}$$

where U_a is the light distribution at the hologram due to the reconstructing source.

$$U_a = A_a(x_1, y_1)e^{j\phi_a(x_1, y_1)} \tag{6}$$

This expression is similar to (1), where now subscript a refers to the reconstructing wave in the hologram plane, but before modulation by the hologram.

Substituting equations 1, 2, 6 into 5 the light distribution leaving the hologram is

$$U = A_a e^{j\phi_a}[A^2_o + A^2_b + A_o A_b e^{j[\phi_o - \phi_b]} + A_o A_b e^{-j[\phi_o - \phi_b]}] \qquad (7)$$

The objective is to choose the reconstructing wavefront U_a, such that when it illuminates the hologram the light distribution leaving the hologram will be like that originally coming from the object U_o. The light distribution leaving the hologram may be considered to consist of three terms

$$\begin{aligned} U = {} & [A^2_o + A^2_b]\, A_a e^{j\phi_a} \\ & + A_o A_b A_a e^{j[\phi_o - \phi_b + \phi_a]} \\ & + A_o A_b A_a e^{-j[\phi_o - \phi_b - \phi_a]} \end{aligned} \qquad (8)$$

The first term is the zero order or essentially a shadowgram of the hologram. The second two terms are the terms of interest and may produce either a real or a virtual image. If in the recording and reconstruction process the following two conditions are imposed:

$$1) \quad A_b e^{j\phi_b} = A_a e^{j\phi_a} \qquad (9)$$

and

$$2) \quad A_b = A_a = \text{constant}$$

the second term in equation (8) except for a constant multiple becomes $A_o e^{j\phi_o}$.

This is a wave exactly like that which came from the object and produces a virtual image [behind the hologram plane] free from aberrations. The last term however becomes a constant times

$$A_o e^{-j[\phi_o - 2\phi_b]} \qquad (10)$$

This wave tends to form a real image in front of the hologram. Note, however, the extraneous phase factor, $(2\phi_b)$. This causes aberrations in the real image, unless it is a constant phase term. Thus, the conditions for obtaining an unaberrated virtual image are, the reconstructing wave and reference wave must be the same form, that is, the reconstructing point source is placed in the same position as the reference source, and $\lambda_1 = \lambda_2$; and the amplitude of the reference wave and reconstructing source should be constant.

From equation (8) it is seen that if

$$A_a e^{j\phi_a} = A_b e^{-j\phi_b}$$

the third term produces a real unaberrated image. This condition means that the reconstructing beam is a mirror image of the reference beam and that $\lambda_1 = \lambda_2$.

One case worth noting is when the reference wave and reconstructing wave are both plane waves and perpendicular to the hologram plate and $\lambda_1 = \lambda_2$. The phase factors ϕ_b and ϕ_a in Equation (8) are then both constant. The last two terms, except for a constant multiplier, then become

$$A_o e^{j\phi_o + c_1} \text{ and } A_o e^{-j\phi_o + c_2}$$

where c_1 and c_2 are constant factors. These produce both a virtual and real image, respectively, exactly like the object and free from all aberrations.

If the wavelength of the source used for reconstructing the image differs from that used when recording the hologram both hologram and reconstructing geometry require scaling factors to reproduce an unaberrated image.

C. OBJECT AND IMAGE POSITIONS

The relationship between the object and image positions can be arrived at as follows. Figure A-2a shows the recording parameters of the hologram. Assume all sources, reference, object and reconstruction beam, to be point sources. Also assume that their amplitudes at the recording plane, while not necessarily equal, are constant. This allows us to deal only with the phases. For simplicity we have assumed the object and reference source to be on the same axis. This produces the Gabor, or in-line type of hologram. The use of the skewed reference beam shifts the image in the x or y dimension but the

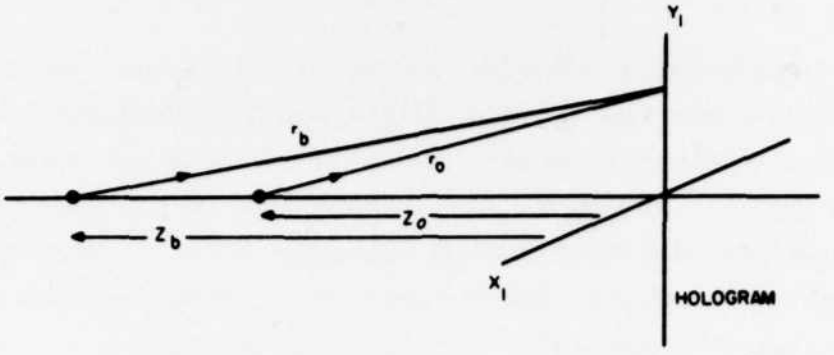

a) Recording

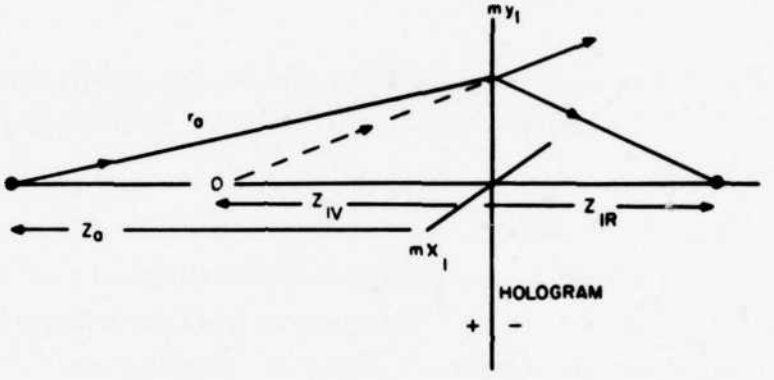

b) Reconstruction

Figure A-2. Recording and Reconstruction Parameters

image position Z_i is the same in either case. The following analysis is easily extended to the off-axis reference beam. It is of interest here to indicate some of the more significant relationships between the image positions and the object, reference beam, and reconstructing source positions and the effects on magnification.

The phase of the light at the hologram plane due to the reference beam is then

$$\phi_b = \frac{2\pi}{\lambda_1} r_b + c \qquad (11)$$

where c represents a constant phase delay. Similar equations can be written for ϕ_o and ϕ_a. Remember that subscripts

b refers to reference beam when recording the hologram.

a refers to the reconstructing beam.

o refers to the object wave.

Substituting into Equation (8) and omitting constant phase delays, the disturbance leaving the hologram is given by

$$U = e^{jk_2 r_a} + e^{j[k_1 r_o - k_1 r_b + k_2 r_a]} + e^{-j[k_1 r_o - k_1 r_b - k_2 r_a]} \tag{12}$$

where

$$k_1 = \frac{2\pi}{\lambda_1}$$

$$k_2 = \frac{2\pi}{\lambda_2}$$

and λ_1 is the recording wavelength and λ_2 is the reconstructing wavelength. The first term is simply the zero order and is of no interest. The last two terms are the image forming waves. Without any loss of generality one can set $x_1 = 0$ and consider only points along the y-axis. The expression for r_b is then

$$r_b = (Z^2_b + y^2_1)^{1/2} \tag{13}$$

Expansion of the square root gives

$$r_b = Z_b + \frac{y^2_1}{2Z_b} - \frac{y^4_1}{8Z^3_b} + \ldots\ldots \tag{14}$$

Similar equations can be written for r_o and r_a. A first order analysis can be performed by neglecting all terms beyond the second term. This is analogous to the relationships derived between object and image positions for ordinary lenses in classical optics. Third order aberrations are arrived at by including

the Z^{-3} term. These effects are discussed later. Making these substitutions the last two terms in Equation (12) can then be written as

$$A_{iV} = \exp. \frac{jk_2 y^2 1}{2} \left[\frac{1}{\mu m^2 Z_o} - \frac{1}{\mu m^2 Z_b} + \frac{1}{Z_a} \right] \tag{15}$$

and

$$A_{iR} = \exp. - \frac{jk_2 y^2 1}{2} \left[\frac{1}{\mu m^2 Z_o} - \frac{1}{\mu_m{}^2 Z_b} - \frac{1}{Z_a} \right] \tag{16}$$

where the constant phase factors $k_1 Z_o$, etc. have been omitted and $\mu = \lambda_1/\lambda_2 = k_2/k_1$, and m is scaling factor which represents the magnification of the hologram before reconstruction. Now let

$$\frac{1}{Z_{iV}} = \left[\frac{1}{Z_a} - \frac{1}{\mu m^2 Z_b} + \frac{1}{\mu m^2 Z_o} \right] \tag{17}$$

and

$$\frac{1}{Z_{iR}} = \left[\frac{1}{Z_a} + \frac{1}{\mu m^2 Z_b} - \frac{1}{\mu m^2 Z_o} \right] \tag{18}$$

substituting into Equation (15) and (16) the two waves leaving the hologram are then

$$A_{iV} = e^{\frac{jk_2 y^2 1}{2 Z_{iV}}} \tag{19}$$

and

$$A_{iR} = e^{\frac{jk_2 y^2 1}{2 Z_{iR}}} \tag{20}$$

These represent two waves emanating from the points Z_{iV}, and Z_{iR}. Thus the distances Z_{iV} and Z_{iR}, as given by Equation (17) and (18), are the locations of the two reconstructed images produced by the hologram. Positive distances are measured to the left of the hologram in Figure A-2 or toward the object source. Thus, positive image distances mean virtual images and negative image distances represent real images. From equations (17) and (18) it

can be seen that Z_{iV} and Z_{iR} may have either positive or negative values depending on the location of the reference source and reconstructing source. That is, either term may be made to produce either a virtual or real image. The case which is generally considered in the literature when describing holography is for $\mu = m = 1$; and $Z_b = Z_a = \infty$. This gives $Z_{iV} = Z_o$ which is the virtual image, and $Z_{iR} = -Z_o$ which is the real image. This is the condition previously described which produces both a real and virtual image exactly like the object.

D. MAGNIFICATION

The lateral magnification may be determined from the geometry used in producing the hologram and in the reconstruction by considering the hologram of a particle to behave like a Fresnel Zone plate. Figure A-3 shows the recording and reconstruction geometry of the hologram. The points x'_1 and x''_1 represent the axis of the zone plates formed by the two particles 0' and 0''.

From the geometry of the figures and Equations (17) and (18)

$$M_V = \frac{S_i}{S_o} = \frac{Z_{iV}}{\mu m Z_o} \tag{21}$$

and

$$M_R = \frac{S_i}{S_o} = -\frac{Z_{iR}}{\mu m Z_o} \tag{22}$$

Note the similarity of these equations to the magnification produced by an ordinary lens. If there is no change of wavelength between recording and reconstruction and no scale change of the hologram, the relationships are identical to those for a thin lens. Substituting for Z_{iV} and Z_{iR} gives the lateral magnification

$$M_{V_{lat}} = m\left[1 + \frac{\mu m^2 Z_o}{Z_a} - \frac{Z_o}{Z_b}\right]^{-1} \tag{23}$$

and

$$M_{R_{lat}} = m\left[1 - \frac{\mu m^2 Z_o}{Z_a} - \frac{Z_o}{Z_b}\right]^{-1} \tag{24}$$

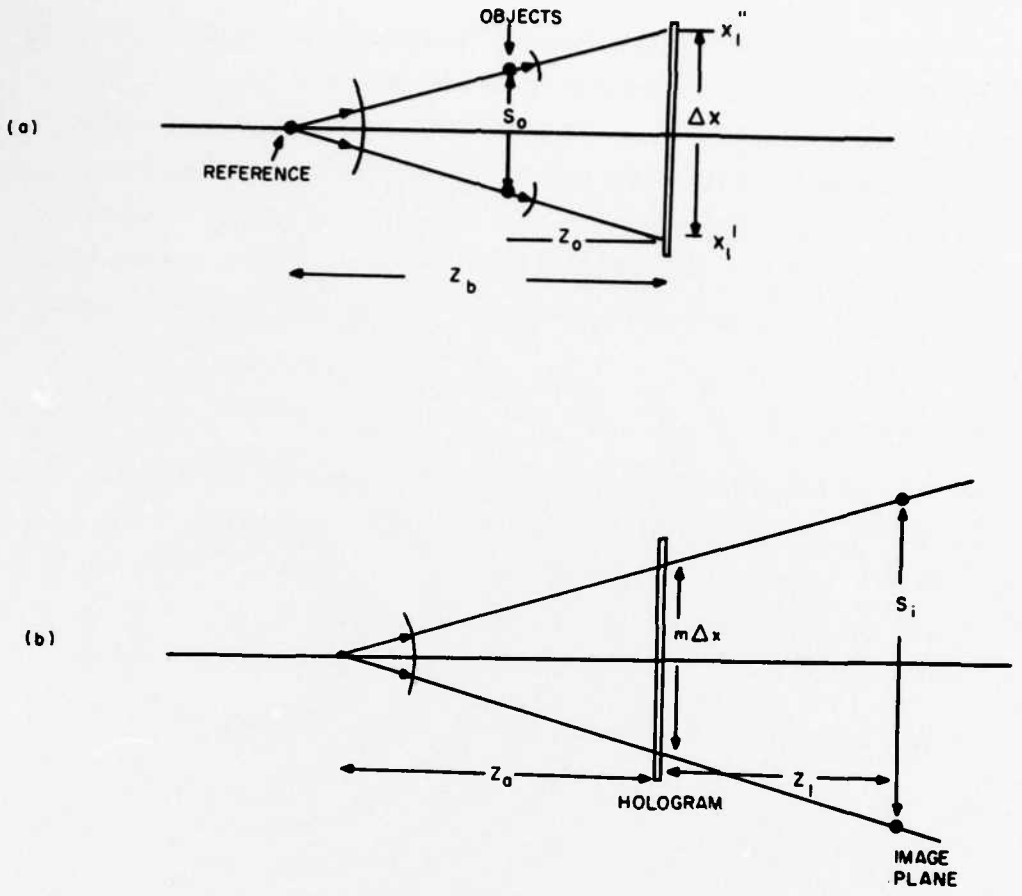

Figure A-3. Magnification Geometry

The longitudinal magnification is

$$M_Z = \frac{d(Z_I)}{d(Z_o)} \tag{25}$$

From Equations (17), (18) and (23), (24) then

$$M_{V_{Long}} = \mu M^2_{V_{lat}} \tag{26}$$

$$M_{R_{Long}} = \mu M^2_{R_{lat}} \tag{27}$$

Or the longitudinal magnification is equal to the lateral magnification squared multiplied by the ratio of recording wavelength to reconstruction wavelength.

Examination of the above equations reveals several interesting situations. If $Z_a = \infty$ e.g., plane wave in reconstruction, then the lateral magnification is independent of any wavelength change. However, the longitudinal magnification is still dependent on both μ and $M^2_{lateral}$ so the image is distorted in depth. It is obvious from Equations (26) and (27) that if the longitudinal magnification is to be equal to the lateral magnification then $M_{lateral} = 1/\mu$. This condition also shows that if there is no wavelength change between recording and reconstruction and the lateral and longitudinal magnification are to be equal then there can be no magnification of either the real or virtual images.

A common configuration for recording holograms is to place the reference source and object at the same distance from the recording plane, e.g., $Z_o = Z_b$. This makes $Z_{iV} = Z_{iR} = Z_a$. Thus the image positions are independent of any wavelength change or scaling factor and both images form in the plane of the reconstructing source. This condition can only be fulfilled for one plane in a three-dimensional object. If undistorted magnification is desired, the lateral magnification should be independent of the object position. From Equations (23) and (24) it can be seen that this condition is satisfied if

$$\frac{Z_a}{Z_b} = \pm\mu m^2 \tag{28}$$

The lateral magnification is then

$$M_{lat} = m$$

The previous condition for equal lateral and longitudinal magnification required $M_{lat} = 1/\mu$. Thus for undistorted magnification the requirements are

$$M_{lat} = m = \lambda_2/\lambda_1 \tag{29}$$

One particular set of conditions which is of special interest is the case where plane wave illumination is used for both the reference and reconstruction

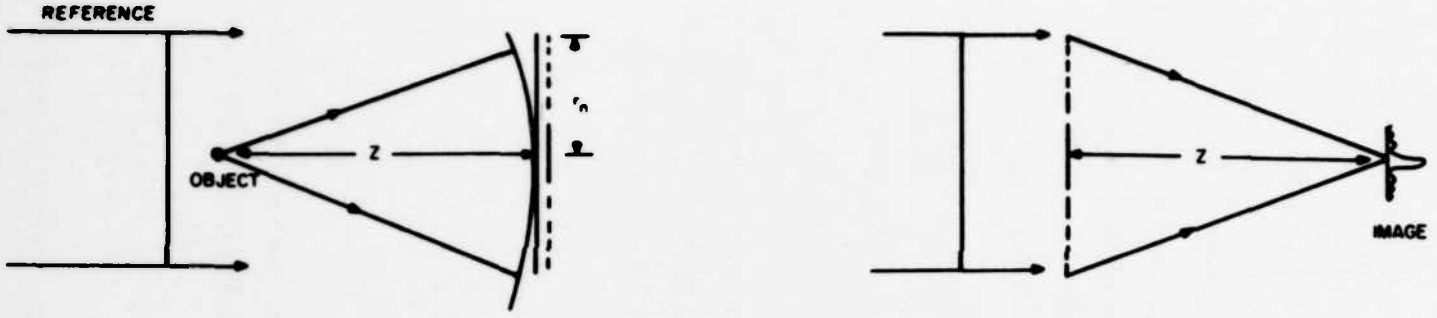

Recording

Reconstruction

Figure A-4. Hologram of a Point

beam, e.g., $Z_b = Z_a = \infty$. Then the lateral magnification is independent of wavelength and $M_V = M_R = m$, the image positions are

$$Z_{iV} = -Z_{iR} = \mu m^2 Z_o \tag{30}$$

If the recording and reconstruction wavelengths are equal and there is no scale change of the hologram then both the real and virtual image have unit magnification in all dimensions and are exactly like the object. This case is an excellent one to work with in practice as it does not require accurate positioning of the hologram either in the recording or reconstruction process.

E. ABERRATIONS

In the above analysis the higher order terms in the expansion of Equation (14) were ignored. If the term in $1/Z^3$ is retained the reconstruction image will have the third order aberrations of coma, spherical aberration, astigmatism, field curvature and distortion. Anyone of these aberrations may be removed by placing appropriate restrictions on the reference and reconstruction beams. However, simultaneous removal of all aberrations requires parallel reference and reconstructing beams and scaling of the hologram according to the wavelength ratio. These conditions were fulfilled in the last case discussed in the preceding section.

F. RESOLUTION

It is well known that the hologram produced by a point source and a plane reference wave is a Fresnel Zone plate. A hologram of an extended object may be considered to be made up of a collection of zone plates from each point on the object. A zone plate consists of a set of alternately opaque and transparent concentric rings whose radii vary as the square root of the integers. See Figure A-4. The radii of the rings are given by

$$r_n^2 = n Z \lambda \tag{31}$$

where r_n is the radius of the nth ring; Z is the distance from the point object to the recording plane which is also the distance from the hologram to the reconstructed image; and n = 1, 2, 3, 4 . . . .

It can be shown that the half-width of the focused spot or light is essentially the same as that for a lens of the same aperture and diameter and is given by

$$\Delta X = \frac{1.22 \lambda Z}{D_N} \tag{32}$$

where

D_N = diameter of nth zone
ΔX = half-width of focused spot

If the Rayliegh criterion is used for defining resolution then ΔX is the closest distance that two spots can be imaged and still be resolved. For plane wave illumination two objects separated by a distance of ΔX will produce zone plates whose axis are also separated by a distance ΔX. Therefore, the resolution of the reconstructed image in lines per unit distance is $1/\Delta X$. If the distance Z is considered to be the focal length of the zone plate then Z/D_n is the f-number of the hologram and the resolution is directly proportional to the f-number.

In order for the film to record a zone plate of Diameter D_n, the film must have a resolution of $2S_n$ where S_n is the width of the last zone. From Equation (31)

$$S_n = \frac{Z\lambda}{r_n + r_{n-1}} \tag{33}$$

If n is large such that $r_n \approx r_{n-1}$

we may write

$$S_n = \frac{Z\lambda}{D_n} \tag{34}$$

and from Equation (32)

$$S_n \cong \Delta X \tag{35}$$

This is a very significant result since it says that the resolution capability of the hologram system is equal to the width of the last zone recorded, and the

film resolution required for recording the hologram must be twice the resolution required of the system. Also implicit in this statement is the fact that the required film resolution is not reduced by recording the hologram at large distances from the object.

The above results give the required film resolution for the on-axis system. In the off-axis system the tilt of the reference beam must be sufficient to remove the image forming waves from the zero-order wave. Considering the hologram of a point as a Fresnel zone plate this means an asymmetrical zone plate will be recorded. In order for the zero-order to be just removed from the image just one side of the zone plate is recorded. In order to maintain resolution the width of the asymmetrical zone plate must be the same as for the on-axis system. This means the radius of the nth zone for the off-axis system is just twice that of the on-axis system and from Equation (33) the width of the nth zone in the off-axis system is just twice that required for the on-axis system. The film resolution then must be four times the resolution required of the on-axis system. If the object consists of a number of points whose maximum separation is b then the zone plate must contain a higher offset or the image of one of the points will fall in the zero order of the other. The radius of the nth zone must then be $[\, b + 2r_n \,]$ when r_n is the radius required for a given resolution for the on-axis system. From equation 33 then the width of the last zone is then

$$S_{n_{offset}} = \frac{Z\lambda}{2b + 2D_N}$$

where

b = width of object

D_N = aperture diameter required to give a resolution ΔX in the on-axis systems.

This result shows that when an offset reference beam is used the minimum resolution required of the recording media is four times the resolution required of the system. If the object has extent, such that its width b is large compared

to D_n, the aperture required to obtain a given resolution, then the film resolution requirements will be determined mainly by the width of the object. The film resolution in lines per mm can be written as

$$\text{off-set film resolution} = \frac{2}{s_{n_{\text{off-set}}}} = \frac{4b}{\lambda Z} + \frac{4}{\Delta X}$$

Note the quantity b/Z is the angle subtended by the object at the recording plane which is to say that if the recording is made at a large distance from the object the film resolution requirements are lowered and approaches $4/\Delta X$. It should be kept in mind however that as the distance Z increases the aperture D_N required to produce a given resolution also increases. If this diameter becomes too large (~ 1 cm.) thickness variations in the film backing will degrade the resolution and a liquid gate will be required in the reconstruction process.

If the film resolution does not meet the system requirements the hologram plane may be magnified before recording. The system resolution will not be degraded provided the magnified hologram contains the same number of zones as the unmagnified version. However as indicated in the previous section scaling of the hologram by a factor of m gives a lateral magnification of m and a longitudinal magnification of m^2 (assuming $\lambda_1 = \lambda_2$) which must be taken into account when making any measurements in the reconstructed image.

G. COHERENCE REQUIREMENTS

As shown in the previous section, the theoretical resolution of the reconstructed image is limited only by the size aperture of the hologram. In practice, however, the storage medium must have the capability of recording the highest spatial frequency in the hologram. This was shown to be just twice the resolution required in the image for the on-axis system. There is a second factor which will also limit the resolution in any practical system and that is the coherence length of the radiation used to record (and reconstruct) the hologram. If the hologram is to have some diameter D_N then the initial source of radiation must have a coherence length which is long enough to produce inter-

ference between the scattered light and the background reference wave, over the entire hologram apreture. For the on-axis reference beam system the coherence length δ is given by (refer to Figure A-5).

$$\delta = \frac{D_N^2}{8Z} \tag{36}$$

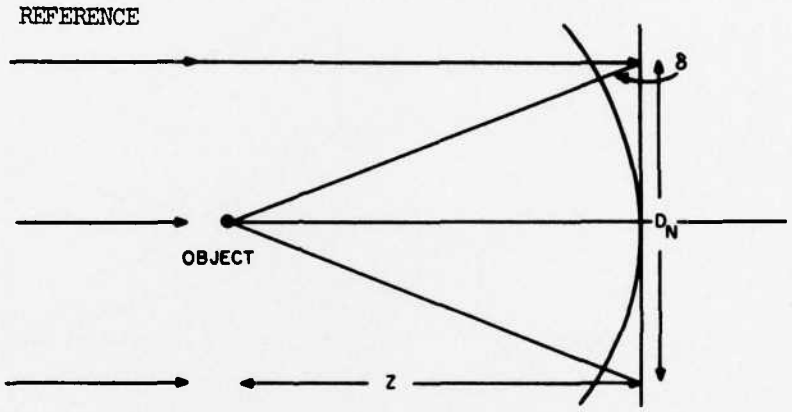

Figure A-5. On-Axis Coherence Requirements

From Equation (32), the coherence length required to give a resolution ΔX is then

$$\delta > \frac{Z}{8} \left(\frac{1.22\lambda}{\Delta X}\right)^2 \tag{37}$$

The coherence length of a laser can be written as

$$\delta = \frac{\bar{\lambda}^2}{\Delta\lambda}$$

where $\bar{\lambda}$ is the center frequency. The required bandwidth of the laser then is

$$\Delta\lambda < \frac{5\Delta X^2}{Z} \tag{38}$$

The above conditions for coherence length are for the on-axis reference beam. The coherence length for the off-axis reference beam can be determined from Figure A-6.

$$\delta \geq r_R - Z$$

$$\delta > \frac{b^2 + 2br_n + r^2_n}{2Z}$$

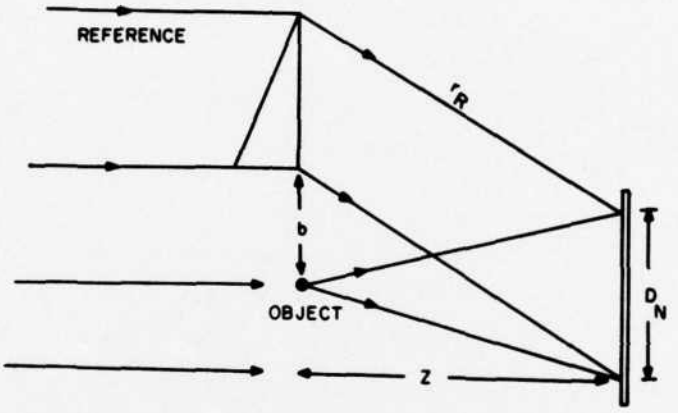

Figure A-6. Off-Axis Coherence Requirements

Obviously the coherence length for the off-axis reference beam, must be greater than that for the on-axis reference beam. This distance must also include any prior path differences due to beam splitters or mirrors used to divert the reference beam around the object.

H. PHOTOGRAPHIC FILM EXPOSURE AND PROCESSING

In Section B it was shown that if the photographic film in which the hologram is stored has an amplitude transmission which is linear with intensity that an image of the object can be reconstructed when the film is re-illuminated with coherent light. It is to be noted here that we are dealing with amplitude transmission of the film and not intensity transmission. If there are

no phase effects in the film due to thickness variation of the emulsion or film backing, the amplitude transmission is just the square root of the intensity transmission. When working with small particles of unknown size and distribution one must be careful to maintain linearity in the recording. Non-linearities in the recording can produce spurious points of light which could be interpreted as particles if the actual particle distribution is not known.

Figure A-7 is a density vs. log exposure curve for Kodak 649F film. From the curve it can be seen that the amplitude transmission of a negative is

$$T_N = KI^{-\gamma/2}$$

where

T_N = amplitude transmission of negative
I = intensity if incident light
K = constant dependent on exposure time
γ = slope in linear region

In order for T_N to be linear with I, requires a negative gamma, which implies a positive transparency. If the negative is contact printed to give a positive transparency the amplitude transmission of the positive is then

$$T_P = K^{1/2} I^{\gamma_N \gamma_P/2}$$

where γ_N and γ_P refer to the gamma of the negative and positive transparency. Thus, if the product $\gamma_N \gamma_P = 2$, the amplitude transmittance of the positive will be linear with intensity.

In practice, however, this overall gamma of two is difficult to achieve and generally because of the high spatial frequencies in the hologram ($\sim$ 2000 lines/mm) it is impossible to copy the negative hologram. This difficulty can be overcome by using the negative transparency and working with the amplitude transmission vs. exposure curve. Figure A-8 shows a plot of amplitude transmission vs. intensity for Kodak 649F film. From this curve it can be seen that there is a considerable region over which the amplitude transmission is linear with intensity.

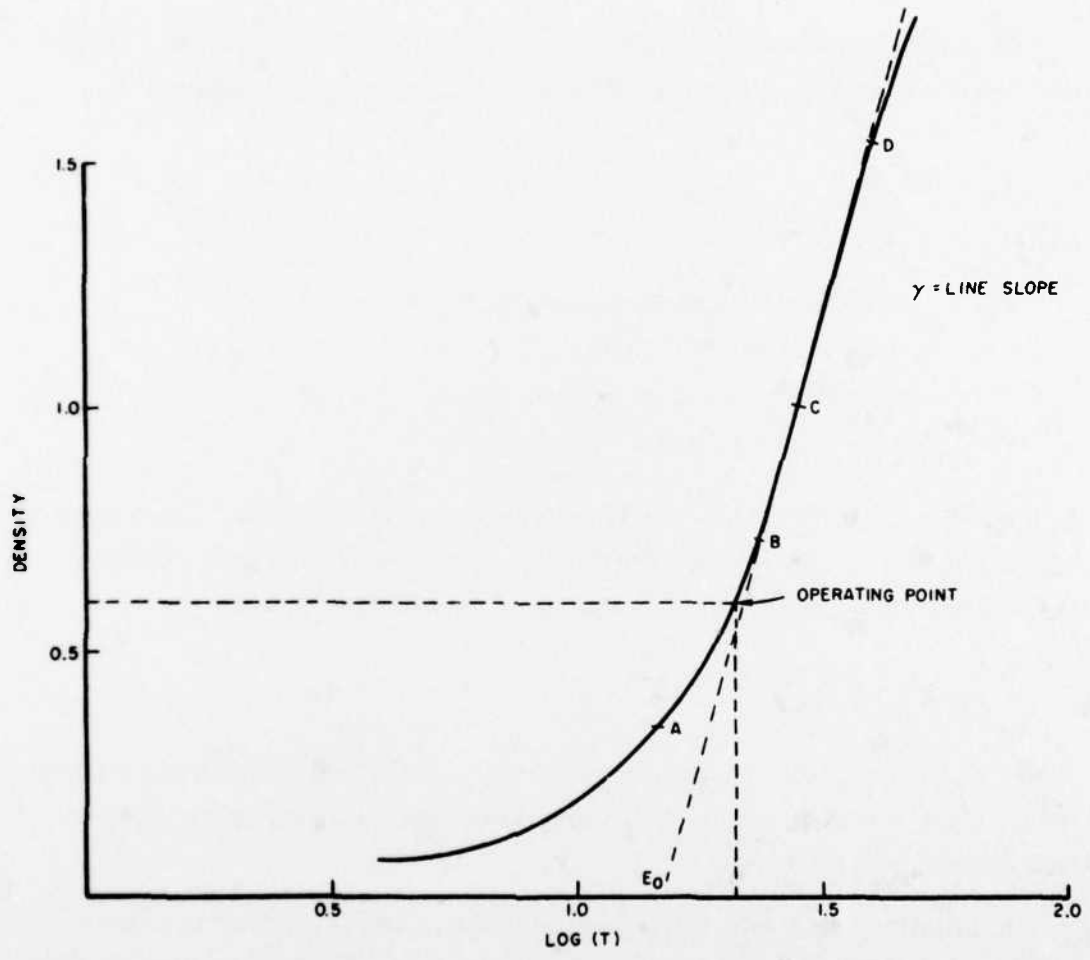

Figure A-7. Density vs. Log Exposure for Kodak 649F

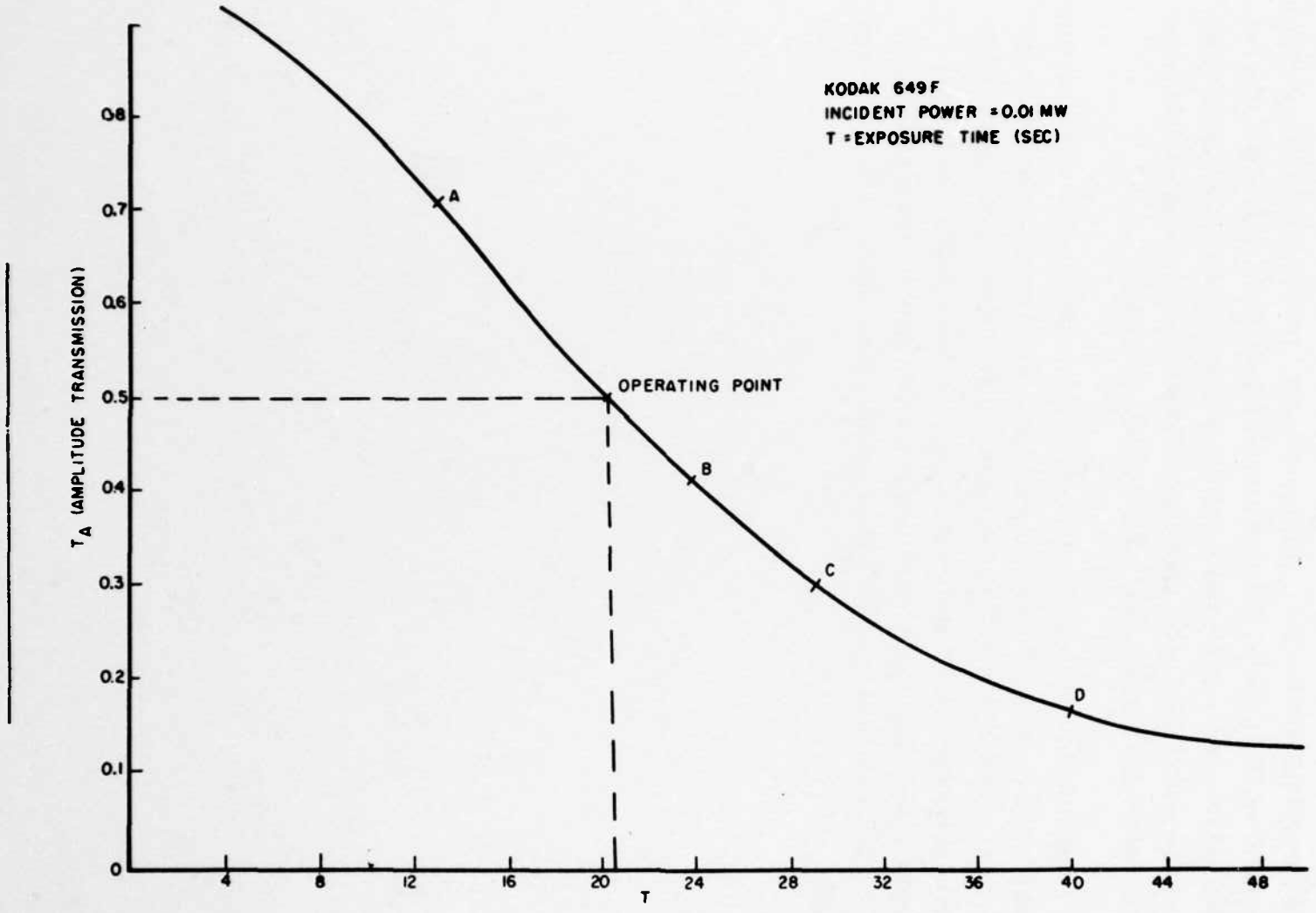

Figure A-8. Amplitude Transmission vs. Exposure for 649F Film

The letters represent corresponding points on the two curves. Note that the linear region on the T vs. E curve does not correspond to the linear region on the D vs. log E curve. Working with the amplitude transmission curve and negative transparencies is convenient since it is a one step process and eliminates the need of copying the hologram. However, care must be taken to maintain linearity in the recording and processing of the film.

Figure A-9 shows the reconstructed image of a set of points where the hologram was purposely recorded non-linearily. For an untrained observer not knowing what the original object consisted of, it is virtually impossible to determine the correct distribution of points. The image should contain only twelve points. The reconstructed image from a linear recording of the same scene is shown in Figure A-10. The bright spot in the center is the zero order light.

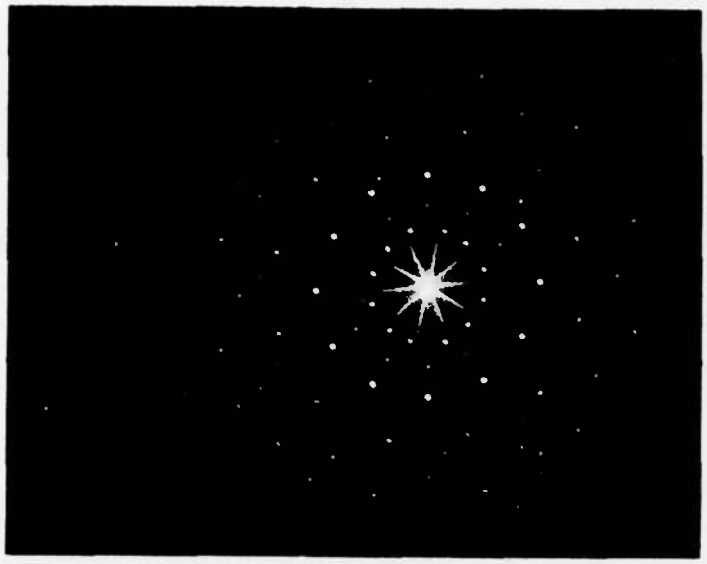

Figure A-9. Reconstructed Image from Nonlinear Recording

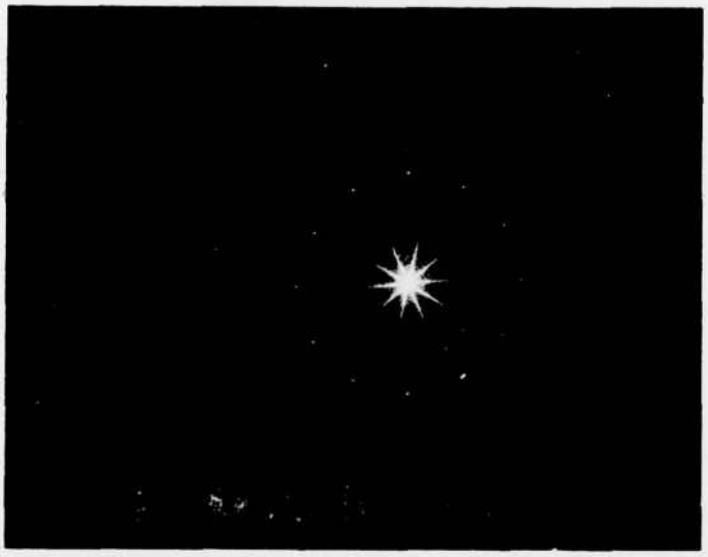

Figure A-10. Reconstructed Image from Linear Recording